SYNTHESIS, CHARACTERIZATION AND STRUCTURAL STUDIES OF MEDICINALLY IMPORTANT PYRIDINE DERIVATIVES

by

ABBAS FARHADIKOUTENAEI

Thesis submitted in fulfillment of the requirements

for the degree of

Doctor of Philosophy

APRIL 2016

ACKNOWLEDGEMENT

I would like to express my sincere gratitude and thanks to my principal supervisor Professor Dr. Abdul Razak Ibrahim, you have been a tremendous adviser, for me during my Ph.D. research. I would also like to acknowledge my co-supervisor Professor Dr. Fun Hoong Kun. I am also grateful to Dr. Thanigaimani Kaliyaperumal who gave me advises on synthesis works. My appreciation is also extended to all the staffs of the Crystallography Laboratory of the School of Physics, Universiti Sains Malaysia. I am very thankful to all my fellow friends in our laboratory at the school of physics for their assistance and guidance during the entire journey to completing this degree. Finally, I would like to thank my wife and my children Soroush & Kiana. Their loving support and patience have made this possible.

TABLE OF CONTENTS

Page

ACKNOWLEDGEMENT ii

TABLE OF CONTENTS iii

LIST OF TABLES x

LIST OF FIGURES xiii

LIST OF ABBREVIATIONS xxv

ABSTRAK xxvii

ABSTRACT xxviii

CHAPTER 1 INTRODUCTION

1.1 Supramolecular Chemistry and Non-covalent Interactions 1

1.2 Supramolecular Architectures 3

1.2.1 Hydrogen Bonding 4

1.2.2 Graph Sets 6

1.3 Crystal Growth 8

1.3.1 Slow Evaporation 9

1.4 Problem Statement 9

1.5 Research Objectives 10

CHAPTER 2 LITERATURE REVIEW

2.1 Hydrogen Bonding Interactions and Supramolecular Chemistry 11

2.2 Study of Powder X-ray Diffraction (PXRD) 20

2.3 Infrared Spectroscopy (IR) 23

2.4 Nuclear Magnetic Resonance (NMR) 25

2.5 Importance of Pyridine and Pyrimidine Derivatives 26

CHAPTER 3 METHODOLOGY

3.1 Introduction 29

3.2 Electromagnetic Spectrum 30

3.3 X-Ray Crystallography 30

3.4 Single Crystal X–Ray Structure Determination 31

3.4.1 Selecting a Sample 31

3.4.2 Data Collection and Data Reduction 33

3.4.3 Data Correction 34

3.4.4 Structure Solution 35

3.4.5 Structure Refinement 36

3.4.6 Software Overview 38

3.5 The Powder Technique 38

3.6 Infrared Spectroscopy 40

3.6.1 The Infrared Absorption Process 42

3.6.2 The Application of Infrared Spectrum 42

3.6.3 IR Sample Preparation (KBr Pellet Method) 43

3.7 Nuclear Magnetic Resonance (NMR) Spectroscopy 44

3.7.1 Chemical Shift in Nuclear Magnetic Resonance (NMR) Spectra 44

3.7.2 Chemical Shift Measurement 45

3.8 Preparation of Samples 46

3.9 Instrumentation 47

3.9.1 Single Crystal X-Ray Diffractometer 47

3.9.2 Powder X-Ray Diffractometer 49

3.9.3 FT-IR Spectrometer....50
3.9.4 NMR Spectrometer....50

CHAPTER 4 RESULTS AND DISCUSSION

4.1 2-Amino-5-methylpyridinium 2-chlorobenzoate 1 52
4.1.1 Molecular Structure....54
4.1.2 Supramolecular Structure 55
4.1.3 IR Spectroscopy 63
4.1.4 NMR Spectroscopy 64
4.2 2-Amino-5-methylpyridinium 3-chlorobenzoate 2 66
4.2.1 Molecular Structure....67
4.2.2 Supramolecular Structure 68
4.2.3 IR Spectroscopy 71
4.2.4 NMR Spectroscopy 73
4.3 2-Amino-5-methylpyridinium 4-chlorobenzoate 3 74
4.3.1 Molecular Structure....75
4.3.2 Supramolecular Structure 77
4.3.3 IR Spectroscopy 80
4.3.4 NMR Spectroscopy 82
4.4 2-Amino-5-methylpyridinium 2-aminobenzoate 4....83
4.4.1 Molecular Structure....84
4.4.2 Supramolecular Structure 85
4.4.3 IR Spectroscopy 90
4.4.4 NMR Spectroscopy 91
4.5 2-Amino-5-methylpyridinium 4-aminobenzoate 5....93
4.5.1 Molecular Structure....94

4.5.2 Supramolecular Structure 95
4.5.3 IR Spectroscopy 98
4.5.4 NMR Spectroscopy 100
4.6 2-Amino-5-methylpyridinium 3-methylbenzoate 6 101
4.6.1 Molecular Structure 103
4.6.2 Supramolecular Structure 103
4.6.3 IR Spectroscopy 108
4.6.4 NMR Spectroscopy 110
4.7 2-Amino-5-methylpyridinium 4-methylbenzoate 7 111
4.7.1 Molecular Structure 113
4.7.2 Supramolecular Structure 114
4.7.3 IR Spectroscopy 117
4.7.4 NMR Spectroscopy 118
4.8 2-Amino-5-methylpyridinium 3-nitrobenzoate 8 119
4.8.1 Molecular Structure 121
4.8.2 Supramolecular Structure 122
4.8.3 IR Spectroscopy 125
4.8.4 NMR Spectroscopy 126
4.9 2-Amino-5-methylpyridinium 4-methoxybenzoate 9 127
4.9.1 Molecular Structure 128
4.9.2 Supramolecular Structure 129
4.9.3 IR Spectroscopy 133
4.9.4 NMR Spectroscopy 134
4.10 2-Amino-5-methylpyridinium 2-(phenylamino)benzoate 10 136
4.10.1 Molecular Structure 137

4.10.2 Supramolecular Structure 138
4.10.3 IR Spectroscopy 142
4.10.4 NMR Spectroscopy 144
4.11 2-Amino-5-methylpyridinium 5-chlorosalicylate 11 145
4.11.1 Molecular Structure 147
4.11.2 Supramolecular Structure 148
4.11.3 IR Spectroscopy 151
4.11.4 NMR Spectroscopy 152
4.12 2-Amino-4-methylpyrimidinium salicylate 12 154
4.12.1 Molecular Structure 155
4.12.2 Supramolcular Structure 156
4.12.3 IR Spectroscopy 160
4.12.4 NMR Spectroscopy 161
4.13 2-Amino-4-methylpyrimidinium 3-methylbenzoate 13 163
4.13.1 Molecular Structure 164
4.13.2 Supramolecular Structure 165
4.13.3 IR Spectroscopy 169
4.13.4 NMR Spectroscopy 170
4.14 2-Amino-4-methylpyrimidinium trifluoroacetate 14 172
4.14.1 Molecular Structure 173
4.14.2 Supramolecular Structure 174
4.14.3 IR Spectroscopy 177
4.14.4 NMR Spectroscopy 179
4.15 2-Amino-4-methylpyrimidinium 2-nitrobenzoate 15 180
4.15.1 Molecular Structure 182

4.15.2 Supramolecular Structure 183
4.15.3 IR Spectroscopy 188
4.15.4 NMR Spectroscopy 189
4.16 2-Amino-4-methylpyrimidinium 5-chlorosalicylate 16 191
4.16.1 Molecular Structure 192
4.16.2 Supramolecular Structure 193
4.16.3 IR Spectroscopy 197
4.16.4 NMR Spectroscopy 198
4.17 2-Amino-4-methylpyrimidinium malonate 17 200
4.17.1 Molecular Structure 201
4.17.2 Supramolecular Structure 202
4.17.3 IR Spectroscopy 205
4.17.4 NMR Spectroscopy 206
4.18 2-Amino-4-methylpyrimidinium phthalate 18 208
4.18.1 Molecular Structure 209
4.18.2 Supramolecular Structure 210
4.18.3 IR Spectroscopy 215
4.18.4 NMR Spectroscopy 217
4.19 2-Amino-4-methylpyrimidiuium phenylacetate 19 218
4.19.1 Molecular Structure 220
4.19.2 Supramolecular Structure 221
4.19.3 IR Spectroscopy 225
4.19.4 NMR Spectroscopy 226
4.20 2-Amino-4-methylpyrimidinium phenoxyacetate 20 228
4.20.1 Molecular Structure 229

4.20.2 Supramolecular Structure 230

4.20.3 IR Spectroscopy 234

4.20.4 NMR Spectroscopy 236

CHAPTER 5 CONCLUSION

5.1 Conclusion……...238

REFERENCES 241

APPENDICES 249

Appendix 1 ^{13}C NMR spectrum of compounds (1-20)

Appendix 2 Geometric parameters

LIST OF PUBLICATIONS

LIST OF TABLES

Page

Table 1.1 Summary of supramolecular interactions (Steed *et al.*, 2007). 4

Table 1.2 Properties of hydrogen bonds (Steed *et al.*, 2007). 5

Table 3.1 Synthesis details 46

Table 4.1 Crystallographic data of compound 1 53

Table 4.2 Hydrogen bonding geometry of compound 1 61

Table 4.3 Experimental vibrational frequency 63

Table 4.4 Crystallographic data for compound 2 66

Table 4.5 Hydrogen bond geometry of compound 2 70

Table 4.6 Experimental vibrational frequency 72

Table 4.7 Crystallographic data for compound 3 75

Table 4.8 Hydrogen bond geometry of compound 3 79

Table 4.9 Experimental vibrational frequency 81

Table 4.10 Crystallographic data for compound 4 83

Table 4.11 Hydrogen bond geometry of compound 4 89

Table 4.12 Experimental vibrational frequency 90

Table 4.13 Crystallographic data for compound 5 93

Table 4.14 Hydrogen bond geometry of compound 5 97

Table 4.15 Experimental vibrational frequency 99

Table 4.16 Crystallographic data for compound 6. 102

Table 4.17 Hydrogen bond geometry of compound 6 107

Table 4.18 Experimental vibrational frequency 109

Table 4.19 Crystallographic data for compound 7 112

Table 4.20 Hydrogen bond geometry of compound 7 116

Table 4.21 Experimental vibrational frequency. 117

Table 4.22 Crystallographic data for compound 8 120

Table 4.23 Hydrogen bond geometry of compound 8 124

Table 4.24 Experimental vibrational frequency. 125

Table 4.25 Crystallographic data for compound 9 128

Table 4.26 Hydrogen bond geometry of compound 9 132

Table 4.27 Experimental vibrational frequency. 133

Table 4.28 Crystallographic data for compound 10..... 136

Table 4.29 Hydrogen bond geometry of compound 10. 141

Table 4.30 Experimental vibrational frequency 143

Table 4.31 Crystallographic data for compound 11..... 146

Table 4.32 Hydrogen bond geometry of compound 11 149

Table 4.33 Experimental vibrational frequency. 151

Table 4.34 Crystallographic data for compound 12..... 154

Table 4.35 Hydrogen bond geometry of compound 12 159

Table 4.36 Experimental vibrational frequency 160

Table 4.37 Crystallographic data for compound 13..... 163

Table 4.38 Hydrogen bond geometry of compound 13 168

Table 4.39 Experimental vibrational frequency 169

Table 4.40 Crystallographic data for compound 14..... 172

Table 4.41 Hydrogen bond geometry of compound 14 176

Table 4.42 Experimental vibrational frequency 178

Table 4.43 Crystallographic data for compound 15..... 181

Table 4.44 Hydrogen bond geometry of compound 15 187

Table 4.45 Experimental vibrational frequency 188

Table 4.46 Crystallographic data for compound 16..... 191

Table 4.47 Hydrogen bond geometry of compound 16 196

Table 4.48 Experimental vibrational frequency 197

Table 4.49 Crystallographic data for compound 17..... 200

Table 4.50 Hydrogen bond geometry of compound 17 204

Table 4.51 Experimental vibrational frequency. 205

Table 4.52 Crystallographic data for compound 18..... 208

Table 4.53 Hydrogen bond geometry of compound 18 214

Table 4.54 Experimental vibrational frequency 216

Table 4.55 Crystallographic data for compound 19..... 219

Table 4.56 Hydrogen bond geometry of compound 19 224

Table 4.57 Experimental vibrational frequency 225

Table 4.58 Crystallographic data for compound 20..... 228

Table 4.59 Hydrogen bond geometry of compound 20 233

Table 4.60 Experimental vibrational frequency 235

LIST OF FIGURES

Page

Figure 1.1 One functional group can form more than one synthon in crystal structures. Three familiar functional groups and their familiar synthons are shown (Tiekink *et al*., 2010). 2

Figure 1.2 A secondary amine donating hydrogen bond to a carbonyl acceptor, (b) the standard way to indicate acceptor and donor atoms (Steed and Atwood, 2009).....5

Figure 1.3 Different types of hydrogen bond geometries: (a) linear, (b) bent, (c) donating bifurcated, (d) accepting bifurcated, (e) trifurcated and (f) three center bifurcated (Steed *et al.*, 2007). 6

Figure 1.4 Constituent of a graph set of $R_2^2(8)$ formed through carboxylic acids (Whitesell, 1999). 7

Figure 1.5 Different types of motif and their graph sets (Whitesell, 1999).....8

Figure 2.1 An ORTEP diagram with the atom labeling scheme. Thermal ellipsoids shown at fifty percent probability. Dashed lines represent hydrogen bonds (Jebas *et al*., 2006). 12

Figure 2.2 Hydrogen bonding pattern, illustrating the fork-like pattern of 2-aminopyridine nicotinic acetate (Jebas *et al*., 2006). 13

Figure 2.3 The 2-amino-3-methylpyridinium and the ortho-phthalate with atom labels, displaying fifty percent probability ellipsoids level. Dashed lines display hydrogen bonds (Jin *et al*., 2001)**.**.....14

Figure 2.4 The asymmetric unit of 2-aminopyridinium and 1-phenylcyclopropane-1-carboxylate, with fifty percent probability ellipsoids level and atoms label for non-hydrogen atoms (He *et al*., 2010).....16

Figure 2.5 Examples of supramolecular homo and hetero synthons: A carboxylic acid homosynthon I, a 2-aminopyridine homosynthon II, 2-aminopyridine-carboxylic acid supramolecular heterosynthon III, and 2-aminopyridinium-carboxylate supramolecular heterosynthon IV (Bis and Zaworotko, 2005).....16

Figure 2.6 A four-component supramolecular (DDAA array) unit that illustrates of type IV heterosynthon and a C—H$\cdots\pi$ interaction in the crystal packing (He *et al*., 2010).....17

Figure 2.7 The molecular configuration and atom-numbering scheme 2-aminopyrimidin-1-ium trichloroacetate, showing fifty percent probability ellipsoids (Hu, 2002). 18

Figure 2.8 Hydrogen bonding interactions in the title salt (Hu, 2002). 18

Figure 2.9 Four possible configurations for adjacent ion-pairs of 2-amino-4-methylpyrimidinium carboxylate in the crystal structures (Aakeröy *et al*., 2003). 19

Figure 2.10 Part of the crystal structure, indicating a helical chain along the *b*-axis. 19

Figure 2.11 PXRD peaks of product and ingredient materials confirm a new phase (Adalder *et al*., 2012). 20

Figure 2.12 The experimental and calculated (obtained from SXRD) PXRD patterns of (2A4MP-2CBA), (2A4MP-4CBA), (2A4MP-3MBA), (2A4MP-4MBA) and their starting materials PXRD patterns (Khalib *et al*., 2014). 22

Figure 2.13 Structure of five organic salts (Jin *et al*., 2011). 23

Figure 2.14 Structure of hydrogen bond synthons (Jin *et al*., 2014). 24

Figure 2.15 The two organic salts with carboxylic acid (Jin *et al*., 2014). 25

Figure 2.16 The structures of pyridine and pyrimidine. 28

Figure 3.1 The experimental arrangement required to the collection of X-ray diffraction data. A crystal is mounted between a source of radiation and a detector (Glusker and Trueblood, 2010). 31

Figure 3.2 The steps of crystal structure determination (Clegg, 1998). 32

Figure 3.3 Diffraction pattern of a single crystal (Vainshtein, 2013). 33

Figure 3.4 The geometry of Bragg-Brentano diffractometer (Dinnebier and Billinge, 2008). 39

Figure 3.5 Example of powder diffraction pattern for TiO_2 nanoparticles (Theivasanthi and Alagar, 2013). 39

Figure 3.6 IR spectrum (Sathyanarayana, 2007). 40

Figure 3.7 The infrared regions of the electromagnetic waves spectrum (Pavia *et al*., 2008). 41

Figure 3.8 The approximate regions of IR spectrum only for stretching vibrations (Pavia *et al*., 2008). 43

Figure 3.9 The NMR signal of TMS isolated in the end of the spectrum (Jacobsen, 2007). 45

Figure 3.10 Images of Bruker SMART APEX II (a) and APEX II DUO (b) system. 48

Figure 3.11 Overview of Bruker D8 Advanced X-Ray Diffractometer. 49

Figure 3.12 PerkinElmer Spotlight 200 FT-IR Spectrometer in USM. 50

Figure 3.13 Bruker Ascend 500 MHz NMR Spectrometer in USM. 51

Figure 4.1 Structure of 2-amino-5-methylpyridinium 2-chlorobenzoate. 52

Figure 4.2 The molecular configuration and atom-numbering of compound 1. 55

Figure 4.3 The crystal structure of the title compound 1 in dimers A, showing a DDAA array. 56

Figure 4.4 N2C—H3NC···O1B and C5B—H5BA···O2C hydrogen bonded, forming an $R_4^2(9)$ ring motif in dimers B & C. 57

Figure 4.5 N2B—H3N···O1C and C5C—H5CA···O2B hydrogen bonded create a 1D chain *via* dimers B & C along [1 0 0]. 57

Figure 4.6 Two chains are linked by C9B—H9BB···O2B hydrogen bonding, making a ribbon-like structure. 58

Figure 4.7 C—H···π interactions in (a), (b) and (c) 59

Figure 4.8 π···π interactions [*symmetry codes* and separation distances; (a) *x*, 1+*y*, *z*; 3.743 Å (b) 1–*x*, 3–*y*, 1–*z*; 3.823 Å] 60

Figure 4.9 The supramolecular architecture of compound 1, viewed along [1 0 0] direction, involving hydrogen bonding (as dashed lines). 61

Figure 4.10 Comparison of PXRD patterns of the salt and the individual components. 62

Figure 4.11 FT-IR spectra of compound 1. 64

Figure 4.12 ^{1}H NMR spectrum of compound 1. 65

Figure 4.13 Structure of 2-amino-5-methylpyridinium 3-chlorobenzoate. 67

Figure 4.14 The molecular configuration and atom-numbering of compound 2. 68

Figure 4.15 (a) The dimmers are linked through N2—H1N2···O1 hydrogen bond, creating 1D chain along [0 0 1]. (b) 2D networks parallel to the *bc*-plane by C2—H2A···O2 hydrogen bond. 69

Figure 4.16 The supramolecular architecture of compound 2, viewed along [0 0 1] direction, involving hydrogen bonding (as dashed lines). 70

Figure 4.17 Comparison of PXRD patterns of the salt and the individual components.....71

Figure 4.18 FT-IR spectrum of compound 2.....72

Figure 4.19 ^{1}H NMR spectrum of compound 2. 74

Figure 4.20 Structure of 2-amino-5-methylpyridinium 4-chlorobenzoate. 74

Figure 4.21 The molecular configuration and atom-numbering of compound 3. 76

Figure 4.22 The dimmers are linked through N2—H1N2···O1 hydrogen bond, generating 1D chain along [0 0 1].....77

Figure 4.23 2D networks parallel to the *bc*-plane by C2—H2A···O2 hydrogen bond.....78

Figure 4.24 Cg1···Cg2 and Cg2···Cg2 interactions.....78

Figure 4.25 The supramolecular architecture of compound 3, viewed along [0 0 1] direction, involving hydrogen bonding (as dashed lines). 79

Figure 4.26 Comparison of PXRD patterns of the salt and the individual components.....80

Figure 4.27 FT-IR spectrum of compound 3.....81

Figure 4.28 ^{1}H NMR spectrum of compound 3. 82

Figure 4.29 Structure of 2-amino-5-methylpyridinium 2-aminobenzoate.....84

Figure 4.30 The molecular configuration and atom-numbering of compound 4. 85

Figure 4.31 The crystal structure of compound 4, illustrates a DDAA array. 86

Figure 4.32 A three-dimensional network is generated by N3—H2N3···O2 hydrogen bonded. 86

Figure 4.33 Part of crystal system shows C—H ···π interaction. 87

Figure 4.34 The supramolecular architecture of compound 4, viewed along [1 0 0] direction, involving hydrogen bonding (as dashed lines). 87

Figure 4.35 π···π interactions [*symmetry codes* and separation distances; (a) *x, y, z*; 3.736 Å (b) 2–*x*, –*y*, –*z*; 3.739 Å]. 88

Figure 4.36 Comparison of PXRD patterns of the salt and the individual components.....89

Figure 4.37 FT-IR spectrum of compound 4.....91

Figure 4.38 ^{1}H NMR spectrum of compound 4. 92

Figure 4.39 Structure of 2-amino-5-methylpyridinium 4-aminobenzoate.....94

Figure 4.40 The molecular configuration and atom-numbering of compound 5. 95

Figure 4.41 Part of the crystal system of compound 5, representing a DDAA array.....96

Figure 4.42 3D networks by N3—H1N3···O1 and N3—H2N3···O2 hydrogen bondings.....96

Figure 4.43 π···π interactions between pyridine rings [*symmetry code* and separation distances; 1–*x*, 1–*y*, 2–*z*; 3.872 Å]. 97

Figure 4.44 Comparison of PXRD patterns of the salt and the individual components.....98

Figure 4.45 FT-IR spectrum of compound 5.....99

Figure 4.46 ^{1}H NMR spectrum of compound 5. 101

Figure 4.47 Structure of 2-amino-5-methylpyridinium 3-methylbenzoate.....101

Figure 4.48 The molecular configuration and atom-numbering of compound 6. 103

Figure 4.49 The dimmers are linked through N2—H1N2···O1 hydrogen bond, creating infinite 1D chain along [0 0 1].....104

Figure 4.50 Part of the crystal structure indicates $R_2^2(14)$ ring motif. 105

Figure 4.51 C2—H2A···O2 H-bond which expands the crystal lattice along [0 1 0] direction. 105

Figure 4.52 (a) and (b) show π–stacking interactions.....106

Figure 4.53 The molecular packing of compound 6, viewed along [1 0 0] direction, involving hydrogen bonding (as dashed lines). 107

Figure 4.54 Comparison of PXRD patterns of the salt and the individual components..... 108

Figure 4.55 FT-IR spectrum of compound 6..... 109

Figure 4.56 ^{1}H NMR spectrum of compound 6. 111

Figure 4.57 Structure of 2-amino-5-methylpyridinium 4-methylbenzoate..... 111

Figure 4.58 The molecular configuration and atom-numbering of compound 7 113

Figure 4.59 The motifs are linked by N2—H1N2···O1 hydrogen bond, creating 1D chain along *c*-axis. 114

Figure 4.60 Part of crystal configuration, representing 2D networks parallel to the *bc*-plane by C2—H2A···O2 hydrogen bond. 115

Figure 4.61 The molecular packing of compound 7, viewed along [0 0 1] direction, involving hydrogen bonding (as dashed lines). 115

Figure 4.62 Comparison of PXRD patterns of the salt and the individual components..... 116

Figure 4.63 FT-IR spectrum of compound 7..... 118

Figure 4.64 ^{1}H NMR spectrum of compound 7. 119

Figure 4.65 Structure of 2-amino-5-methylpyridinium 3-nitrobenzoate. 119

Figure 4.66 The molecular configuration and atom-numbering of compound 8 121

Figure 4.67 N—H···O hydrogen bond, forming 1D chain along *b*-axis. 122

Figure 4.68 The chain also has C—H···O hydrogen bonded. 123

Figure 4.69 Weak π–stacking interactions [*symmetry code* and separation distance; 1–*x*, –*y*, 1–*z*; 3.907 Å]..... 123

Figure 4.70 Comparison of PXRD patterns of the salt and the individual components..... 124

Figure 4.71 FT-IR spectrum of compound 8..... 126

Figure 4.72 ^{1}H NMR spectrum of compound 8. 127

Figure 4.73 Structure of 2-amino-5-methylpyridinium 4-methoxybenzoate. 127

Figure 4.74 The molecular configuration and atom-numbering of compound 9. 129

Figure 4.75 The crystal lattice of compound 9, illustrates a DDAA array *via* N—H···O hydrogen bonding. 130

Figure 4.76 π–stacking between cations and anions. 131

Figure 4.77 The molecular structure of compound 9 viewed along [1 0 0] direction, involving hydrogen bonding (as dashed lines). 131

Figure 4.78 Comparison of PXRD patterns of the salt and the individual components. 132

Figure 4.79 FT-IR spectrum of compound 9. 134

Figure 4.80 ^{1}H NMR spectrum of compound 9. 135

Figure 4.81 Structure of 2-amino-5-methylpyridinium 2-(phenylamino)benzoate. 137

Figure 4.82 The crystal configuration and atom-numbering of compound 10. . 138

Figure 4.83 The motifs are linked by N2—H1N2···O2 hydrogen bond, creating 1D chain along [0 1 0]. 139

Figure 4.84 Part of crystal packing shows (a) C3—H3A···Cg1 and (b) C11—H11A···Cg3 interactions. 140

Figure 4.85 π–stacking between pyridine and benzene rings. 141

Figure 4.86 Comparison of PXRD patterns of the salt and the individual components. 142

Figure 4.87 FT-IR spectrum of compound 10. 143

Figure 4.88 ^{1}H NMR spectrum of compound 10. 145

Figure 4.89 Structure of 2-amino-5-methylpyridinium 5-chlorosalicylate. 145

Figure 4.90 The crystal configuration and atom-numbering of compound 11. . 147

Figure 4.91 The synthons are linked by N2—H1N2···O2 hydrogen bond, creating 1D chain along [0 1 0] direction. 148

Figure 4.92 2D networks parallel to (1 0 1) Plane *via* C10—H10A···O3 hydrogen bond. 149

Figure 4.93 Comparison of PXRD patterns of the salt and the individual components.....150

Figure 4.94 FT-IR spectrum of compound 11.....152

Figure 4.95 ^{1}H NMR spectrum of compound 11. 153

Figure 4.96 Structure of 2-amino-4-methylpyrimidinium salicylate.....155

Figure 4.97 The crystal configuration and atom-numbering of compound 12. .156

Figure 4.98 The heterosynthons are linked by N2—H1N2···O2 H-bond, creating cyclic heterotetramer. 157

Figure 4.99 π···π interactions between pyrimidine and benzene rings [*symmetry code* and separation distances; 2–*x*, 3/2–*y*, *z*; 3.579 Å]. 157

Figure 4.100 Part of crystal structure shows C—H···π interactions [*symmetry code*: 2–*x*, 1–*y*, –*z*]. 158

Figure 4.101 The molecular structure of compound 12, viewed along [0 1 0] direction, involving hydrogen bonding (as dashed lines). 158

Figure 4.102 Comparison of PXRD patterns of the salt and the individual components.....159

Figure 4.103 FT-IR spectrum of compound 12.....161

Figure 4.104 ^{1}H NMR spectrum of compound 12. 162

Figure 4.105 Structure of 2-amino-4-methylpyrimidinium 3-methylbenzoate....164

Figure 4.106 The crystal configuration and atom-numbering of compound 13. .165

Figure 4.107 Part of the crystal packing of compound 13, showing the configuration of a zig-zag chain along the *b*-axis.....166

Figure 4.108 The C—H···π interaction between the chains. 166

Figure 4.109 The π···π interaction between benzene and pyrimidine rings along [1 0 0] direction. 167

Figure 4.110 The molecular packing of the compound 13. 167

Figure 4.111 Comparison of PXRD patterns of the salt and the individual components.....168

Figure 4.112 FT-IR spectrum of compound 13.....170

Figure 4.113 ^{1}H NMR spectrum of compound 13. 171

Figure 4.114 Structure of 2-amino-4-methylpyrimidinium trifluoroacetate..... 173

Figure 4.115 The crystal configuration and atom-numbering of compound 14. . 174

Figure 4.116 Infinite chain along *a*-axis. 175

Figure 4.117 π···π stacking interactions, cations are related by an inversion center. 175

Figure 4.118 The molecular structure of compound 14, viewed along [1 0 0] direction, involving hydrogen bonding (as dashed lines). 176

Figure 4.119 Comparison of PXRD patterns of the salt and the individual components. 177

Figure 4.120 FT-IR spectrum of compound 14. 178

Figure 4.121 ^{1}H NMR spectrum of compound 14. 180

Figure 4.122 Structure of 2-amino-4-methylpyrimidinium 2-nitrobenzoate. 180

Figure 4.123 The crystal configuration and atom-numbering of compound 15. . 182

Figure 4.124 The crystal lattice of the compound 15, showing a DDAA array... 184

Figure 4.125 C4—H4A···O1 H-bond, which leads to 1D chain along [1 0 1].... 184

Figure 4.126 C12—H12A···O2 H-bond, which forms 2D networks parallel to the *ac*-plane. 185

Figure 4.127 Part of molecular configuration indicates C—H···π interactions... 185

Figure 4.128 Part of molecular packing represents π···π interactions. 186

Figure 4.129 The molecular packing of compound 15, viewed along *b*-axis, involving hydrogen bonding (as dashed lines). 186

Figure 4.130 Comparison of PXRD patterns of the salt and the individual components. 187

Figure 4.131 FT-IR spectrum of compound 15. 189

Figure 4.132 ^{1}H NMR spectrum of compound 15. 190

Figure 4.133 Structure of 2-amino-4-methylpyrimidinium 5-chlorosalicylate.... 192

Figure 4.134 The crystal configuration and atom-numbering of compound 16. . 193

Figure 4.135 The crystal lattice of the compound 16, showing a DDAA array... 194

Figure 4.136 C4—H4A···O3 H-bond, which leads to 1D chain along [2 1 0] direction with an $R_4^4(18)$ ring motif. 194

Figure 4.137 Part of molecular packing illustrates π···π interactions. 195

Figure 4.138 The molecular configuration of compound 16, viewed along [1 0 0] direction, involving hydrogen bonding (as dashed lines). 195

Figure 4.139 Comparison of PXRD patterns of the salt and the individual components..... 196

Figure 4.140 FT-IR spectrum of compound 16..... 198

Figure 4.141 ^{1}H NMR spectrum of compound 16. 199

Figure 4.142 Structure of 2-amino-4-methylpyrimidinium malonate. 201

Figure 4.143 The crystal configuration and atom-numbering of compound 17. Atoms H5AA and H7AA are at the symmetry positions of (*x*, 3/2–*y*, *z*). 202

Figure 4.144 N2—H1N2···O1 H-bond, which builds up 1D chains along [1 0 0] direction..... 203

Figure 4.145 C5—H5B···O3 H-bond, which generates 2D networks parallel to the *ac*-plane. 203

Figure 4.146 Comparison of PXRD patterns of the salt and the individual components..... 204

Figure 4.147 FT-IR spectrum of compound 17..... 206

Figure 4.148 ^{1}H NMR spectrum of compound 17. 207

Figure 4.149 Structure of 2-amino-4-methylpyrimidinium phthalate. 209

Figure 4.150 The crystal configuration and atom-numbering of compound 18. . 210

Figure 4.151 N—H···N hydrogen bond builds up homosynthon ring motif. 211

Figure 4.152 C2B—H2BA···O4B hydrogen bond, which generates 3D networks..... 212

Figure 4.153 Part of crystal configuration represents C—H···π interaction. 212

Figure 4.154 π···π interaction between anions and cations 213

Figure 4.155 π···π interaction between neutral and protonated pyrimidine rings [*symmetry code*: 1+*x*, 3/2−*y*, 1/2+z]. 213

Figure 4.156 The molecular configuration of compound 18, viewed along [1 0 0] direction, involving hydrogen bonding (as dashed lines). 214

Figure 4.157 Comparison of PXRD patterns of the salt and the individual components. 215

Figure 4.158 FT-IR spectrum of compound 18. 216

Figure 4.159 ^{1}H NMR spectrum of compound 18. 218

Figure 4.160 Structure of 2-amino-4-methylpyrimidinium phenylacetate. 218

Figure 4.161 The crystal configuration and atom-numbering of compound 19. . 220

Figure 4.162 N2—H1N2···O1 hydrogen bond, building up a chain along [0 1 0]. 221

Figure 4.163 A chain of $R_3^2(9)$ is generated through C4—H4A···N3 H-bond together with N2—H1N2···O1 H-bond. 222

Figure 4.164 C5—H5C···O2 hydrogen bonds form the rungs of the ladder. 222

Figure 4.165 Part of crystal architecture shows C5—H5B···Cg1 and 223

Figure 4.166 The molecular system of compound 19, viewed along [0 1 0] direction, involving hydrogen bonding (as dashed lines). 223

Figure 4.167 Comparison of PXRD patterns of the salt and the individual components. 224

Figure 4.168 FT-IR spectrum of compound 19. 226

Figure 4.169 ^{1}H NMR spectrum of compound 19. 227

Figure 4.170 Structure of 2-amino-4-methylpyrimidinium phenoxyacetate. 229

Figure 4.171 The crystal configuration and atom-numbering of compound 20. . 230

Figure 4.172 N2—H1N2···O1 H-bond, building up a chain along [0 0 1]. 231

Figure 4.173 A chain of $R_3^2(11)$ is created by C9—H9A···O2 H-bond together with N2—H1N2···O1 H-bond. 231

Figure 4.174 Part of crystal system indicates C—H···π interaction. 232

Figure 4.175 Part of crystal system indicates π···π interaction. 232

Figure 4.176 The molecular system of compound 20, viewed along [0 0 1] direction, involving hydrogen bonding (as dashed lines). 233

Figure 4.177 Comparison of PXRD patternsof the salt and the individual components..... 234

Figure 4.178 FT-IR spectrum of compound 20..... 235

Figure 4.179 ^{1}H NMR spectrum of compound 20. 237

LIST OF ABBREVIATIONS

2A4MP	2-Amino-4-methylpyrimidine
2A5MP	2-Amino-5-methylpyridine
2ABA	2-Aminobenzoic Acid
2CBA	2-Chlorobenzoic Acid
2NBA	2-Nitrobenzoic Acid
3CBA	3-Chlorobenzoic Acid
3MBA	3-Methylbenzoic Acid
3NBA	3-Nitrobenzoic Acid
4ABA	4-Aminobenzoic Acid
4CBA	4-Chlorobenzoic Acid
4MBA	4-Methylbenzoic Acid
4MOBA	4-Methoxybenzoic Acid
5CHS	5-Chlorosalicylic Acid
DMSO	Dimethyl Sulfoxide
MA	Malonic Acid
NPHTA	N-Phenylanthranilic Acid
ORTEP	Oak Ridge Thermal Ellipsoid Plot
PAA	Phenylacetic Acid
PHT	Phthalic Acid
POA	Phenoxyacetic acid
PPm	Part Per million
SADABS	Siemens Area Detector Absorption Correction
SAINT	Siemens Analytical X-ray Area Detector Integration

SALA	Salicylic Acid
SIMU	Simulation
SMART	Siemens Molecular Analysis Research Tools
TFA	Trifluoroacetic Acid
TMS	Tetramethylsilane

SINTESIS, PENCIRIAN DAN KAJIAN STRUKTUR TERBITAN PIRIDIN BERKEPENTINGAN PERUBATAN

ABSTRAK

Dalam kajian ini, dua puluh garam 2-amino-5-metilpiridin dan 2-amino-4-metilpirimidin dengan asid karboksilik aromatik dan alifatik asli telah dikaji menggunakan kaedah spektroskopik seperti: kristalografi sinar-X serbuk dan hablur tunggal, spektroskopi inframerah (IR) dan resonan magnet nuklear (NMR). Dalam semua sebatian, N yang diprotonkan dan kumpulan 2-amino kation terikat dengan ikatan hidrogen kepada atom O karboksilat anion melalui sepasang ikatan hydrogen N–H···O dan N^{+}–H···O^{-}, membentuk motif gelang $R_2^2(8)$. Penghalusan struktur menunjukkan yang empat belas dari sebatian menghablur dalam kumpulan ruang monoklinik, empat dalam triklinik dan setiap satu dalam tetragonal dan ortorombik. Dalam kajian ini, pembentukan hablur ditunjukkan oleh persetujuan yang baik antara corak belauan serbuk sampel dan corak simulasi dari data belauan hablur tunggal dan kedua-duanya berbeza dari corak serbuk bahan awal. Dalam semua sebatian, ikatan kombinasi N—H dalam piridin dan pirimidin ditunjukkan oleh puncak yang berhubungan kepada frekuensi terikan 1877 sehingga 2044 cm^{-1} dan ion karboksilat dicirikan oleh frekuensi terikan asimetrik dan simetrik dalam kawasan 1550–1650 dan sekitar 1400 cm^{-1}, setiap satunya. Pemindahan proton dan tulang belakang semua sebatian juga telah dianalisis menggunakan ^{1}H NMR dan ^{13}C NMR.

SYNTHESIS, CHARACTERIZATION AND STRUCTURAL STUDIES OF MEDICINALLY IMPORTANT PYRIDINE DERIVATIVES

ABSTRACT

In this work, twenty novel salts of 2-amino-5-methylpyridine and 2-amino-4-methylpyrimidine with aromatic and aliphatic carboxylic acids have been investigated using spectroscopic methods such as powder and single crystal X-ray crystallography, infrared (IR) and nuclear magnetic resonance (NMR) spectroscopy. In all the compounds, the protonated N atom and the 2-amino group of the cations are hydrogen bonded to the carboxylate O atoms of the anions *via* a pair of N–H···O and N^{+}–H···O^{-} hydrogen bonds, forming an $R_2^2(8)$ ring motifs. The refinement of the structures indicates that fourteen of the compounds crystallized in the monoclinic space group, four in triclinic and one each in tetragonal and orthorhombic. In this research, the formation of the new crystal is shown by a good consistency between the powder diffraction pattern of the bulk samples and the simulated patterns obtained from single X-ray diffraction data and they were different from the powder pattern of the starting materials. In all the compounds, the combination bond of the N–H in pyridine and pyrimidine was shown by the peaks related to stretching frequencies of 1877 to 2044 cm^{-1} and the ion of carboxylate is characterized by asymmetrical and symmetrical stretching frequencies in the region of 1550–1650 and about 1400 cm^{-1}, respectively. The proton transfer and the skeleton for all the compounds were also analyzed by ^{1}H NMR and ^{13}C NMR.

CHAPTER 1

INTRODUCTION

1.1 Supramolecular Chemistry and Non-covalent Interactions

The phrase supramolecular chemistry has been described by Jean-Marie Lehn who has won the Nobel Prize in the research of "the chemistry of the intermolecular bond and of the molecular assemblies" (Lehn, 1978). Noncovalent forces are the fundamental tool for both supramolecular chemistry and crystal engineering (Desiraju, 2002; Rao, 2001). Investigation about supramolecular chemistry was initially inspired by the tendency to understand the formation of electrical phenomena *via* potassium and sodium ion carried in the nervous system (Lehn, 1988). In 1967, Pedersen constructed a seminal contribution to this interest area in his report that macrocyclic crown ethers are able to bind metal cations such as potassium. Besides the research done by Pedersen (1967), seminal contributions by Boenigk (1988) on spherands and Lehn (1988) on cryptands promoted the conception of self-assembly and molecular recognition as an area of scientific research. Modern-day supramolecular chemistry intersects with several interdisciplinary research fields that bridges other sciences like chemistry, biology, and physics (Steed and Atwood, 2009). In general, supramolecular chemistry refers to the branch of chemistry that deals with the design and fabrication of great and complex supermolecular assemblies by a series of non-covalent bonding events that include intermolecular interactions between the components (Dunitz, 1991). While molecules are made with covalent bonds, supramolecular compounds are made by joining molecules through intermolecular interactions.

The reactivity between molecules depends on the functional groups, such as carboxamide, phenol, amine, alcohol, aniline, aromatic, halogen and carboxylic acid. Therefore, recognition of the functional group gives information about interactions and productions of compounds in a specified category (Carey and Sundberg, 2007). However, in supramolecular system the behavior of a certain functional group is not simply extracted. For instance, carboxylic acids not only constitute expected dimer but also form hydrogen bonding catemer and hydrogen ring motifs (Figure 1.1).

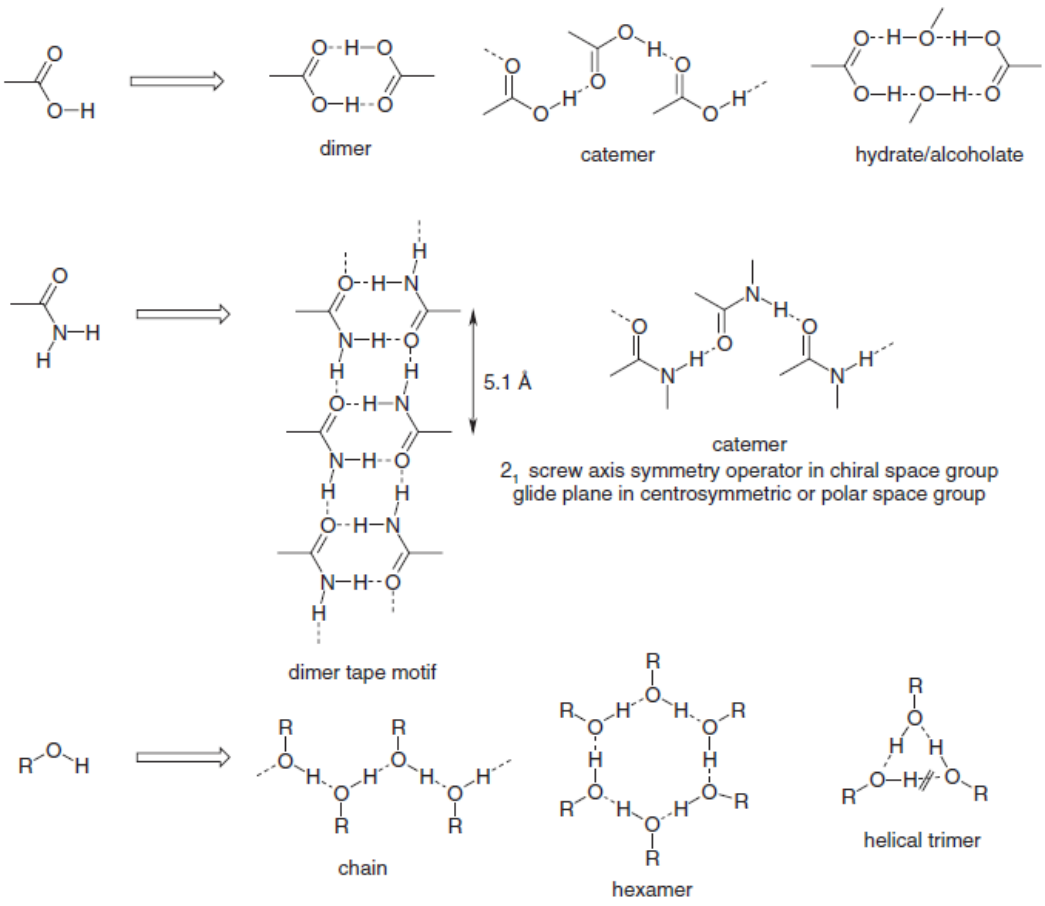

Figure 1.1 One functional group can form more than one synthon in crystal structures. Three familiar functional groups and their familiar synthons are shown (Tiekink *et al.*, 2010).

In the solid state, differently assembled patterns of functional groups have been called supramolecular synthons (Steed and Atwood, 2009). Generally, the functional group of COOH is connected to the finite dimer synthon but sometimes infinite catemers are formed.

1.2 Supramolecular Architectures

In general, supramolecular chemistry is described by non-covalent interactions. Non-covalent interactions indicate the energies that keep supramolecular system together. The term non-covalent includes an immense range of attractions and repulsions effects which are summarized in Table 1.1 (Steed *et al*., 2007).

In the area of supramolecular chemistry, the controlled formation of atoms and molecules *via* reversible linkage like hydrogen bonding, Van der Waals forces, π–π stacking and etc is delved, and many organized architectures have been made by using molecular building blocks (Lingenfelder *et al*., 2004).

Organic crystal structures formed from acid-base compounds have received particular attention in the predictable formation of supramolecular architectures (Shan *et al*., 2003). Self-organization is one of the important methods to create one, two or three-dimensional networks through O—H···O, N—H···O and other weak intermolecular forces (Li *et al*., 2007). Aromatic acids are important in crystal engineering because they can form directional and strong hydrogen bonds (Bhogala and Nangia, 2003), also the number and different location of the carboxylic groups in an aromatic ring can give rise to different types of hydrogen bond and architecture (Zhang and Chen, 2005).

Table 1.1 Summary of supramolecular interactions (Steed *et al*., 2007).

Interaction	Strength (kJ/mol)
ion–ion	200 – 300
Ion - dipole	50 – 200
Dipole - dipole	5 – 50
Hydrogen bonding	4 – 120
Cation–π	5 – 80
π–π	0 – 50
Van der Waals	< 5 (kJ/mol) but variable depending on surface area
Hydrophobic	Related to solvent–solvent interaction energy

1.2.1 Hydrogen Bonding

The hydrogen bonding was discovered about hundred years ago (Steiner, 2002), but still is a subject of very important scientific research. The hydrogen bond, due to high degree of directionality and strength is the most important non-covalent interaction. It states a particular type of dipole-dipole interaction between a donor (D) and an acceptor (A), *via* an intermediate atom of hydrogen (Vilar *et al*., 2004). In this process, the hydrogen atom is covalently bound with an extremely electronegative atom such as nitrogen (N), oxygen (O) or fluorine (F), as the donor. The electron density of the covalent bond is shifted to the donor atom; hence, a partial positive charge (net atomic charge) is created on the hydrogen atom. This charge interacts with the electron cloud around the acceptor (Torshin *et al*., 2002). Hydrogen bond is generally written as D–H···A. A typical hydrogen bond is shown in Figure 1.2.

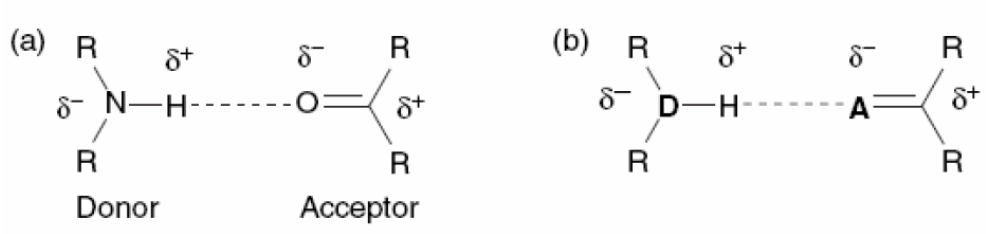

Figure 1.2 A secondary amine donating hydrogen bond to a carbonyl acceptor, (b) the standard way to indicate acceptor and donor atoms (Steed and Atwood, 2009)

There are also important hydrogen bond interactions connecting hydrogen atoms attached to carbon, instead of electronegative atoms such as nitrogen and oxygen (Jeffrey and Jeffrey, 1997). A bond between carbon and hydrogen is the carbon hydrogen bond (C–H) that can be seen in many organic structures (March, 1992). The strength of hydrogen bonds is very different in various systems. It depends on the electronegativity of the donor atom and the geometry of hydrogen bond in the structure. Hydrogen bonds usually appear in a broad range of geometries, lengths and strengths that can be classified into three wide categories, Table 1.2 shows their properties.

Table 1.2 Properties of hydrogen bonds (Steed *et al*., 2007).

	Strong	Moderate	Weak
Type of bonding	Mostly covalent	Mostly electrostatic	Electrostatic
H-bond (Å)	1.2–1.5	1.5–2.2	2.2–3.2
Bond angle (°)	175–180	130–180	90–150
Bond energy (kJ/mol)	14–40	4–15	< 4

The types of geometries of the hydrogen bondings are summarized in Figure 1.3. These geometries of hydrogen bond are called *primary hydrogen bond interactions*, because a direct interaction occurs between donor and acceptor group (Steed and Atwood, 2009).

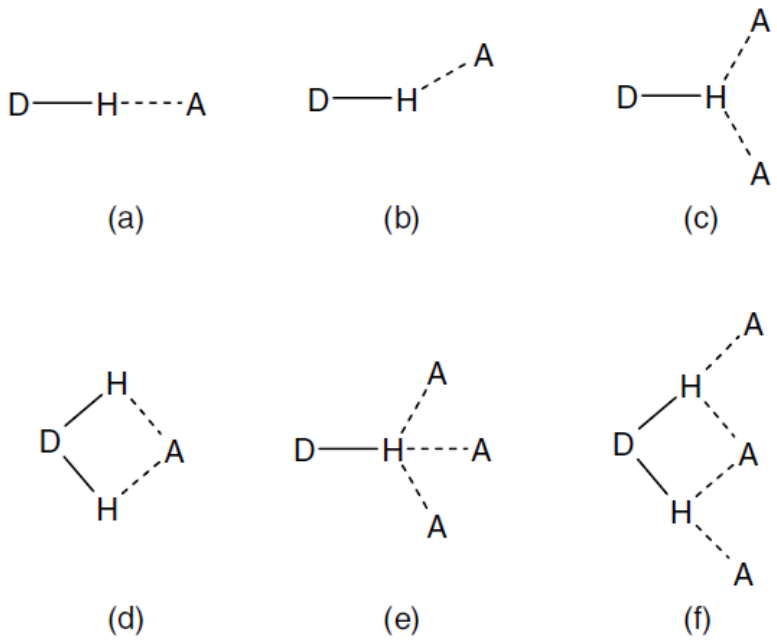

Figure 1.3 Different types of hydrogen bond geometries: (a) linear, (b) bent, (c) donating bifurcated, (d) accepting bifurcated, (e) trifurcated and (f) three center bifurcated (Steed *et al.*, 2007).

1.2.2 Graph Sets

Etter (1985) presented a simple and general method for characterizing, comparing and recognizing patterns of hydrogen bonding in molecular aggregates. All types of hydrogen bonds have been defined just by four simple motifs. The aim of graph set designator is to describe the similarities and differences of hydrogen-bonded arrays (Etter, 1990). The process of specifying a graph set is determined by identifying the various types of hydrogen bonds present in a given network and the molecular structures of acceptors and donors (Chin *et al.*, 1999). The pattern formed through

hydrogen-bonded set by only one type of hydrogen bond is called a motif (Etter *et al*., 1990). A motif has one of four designators based on if the hydrogen bonds are intramolecular or intermolecular. Intermolecular hydrogen bonds generate ring (R), chain (C) and dimer (D) motifs. A self (S) motif is formed from intramolecular hydrogen bond. The repeating motifs due to hydrogen-bonding is specified by the following symbolization (Blagden *et al*., 1998):

$$G_d^a(n)$$

Where, G represents the motifs that can be C, R or S, *a* and *d* are the numbers of acceptor and donors, respectively, and *n* is the number of atoms included within the motif.

The subscript (*d*) and the superscript (*a*) can be dropped whilst both values are one. The method of assigning an eight-membered graph-set formed with carboxylic acids is illustrated in Figure 1.4. Different types of motifs by their graph sets are shown in Figure 1.5 (Chin *et al*., 1999).

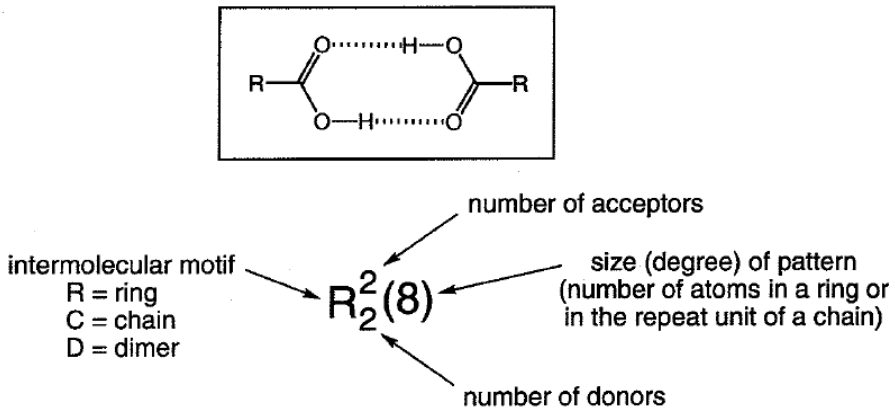

Figure 1.4 Constituent of a graph set of $R_2^2(8)$ formed through carboxylic acids (Whitesell, 1999).

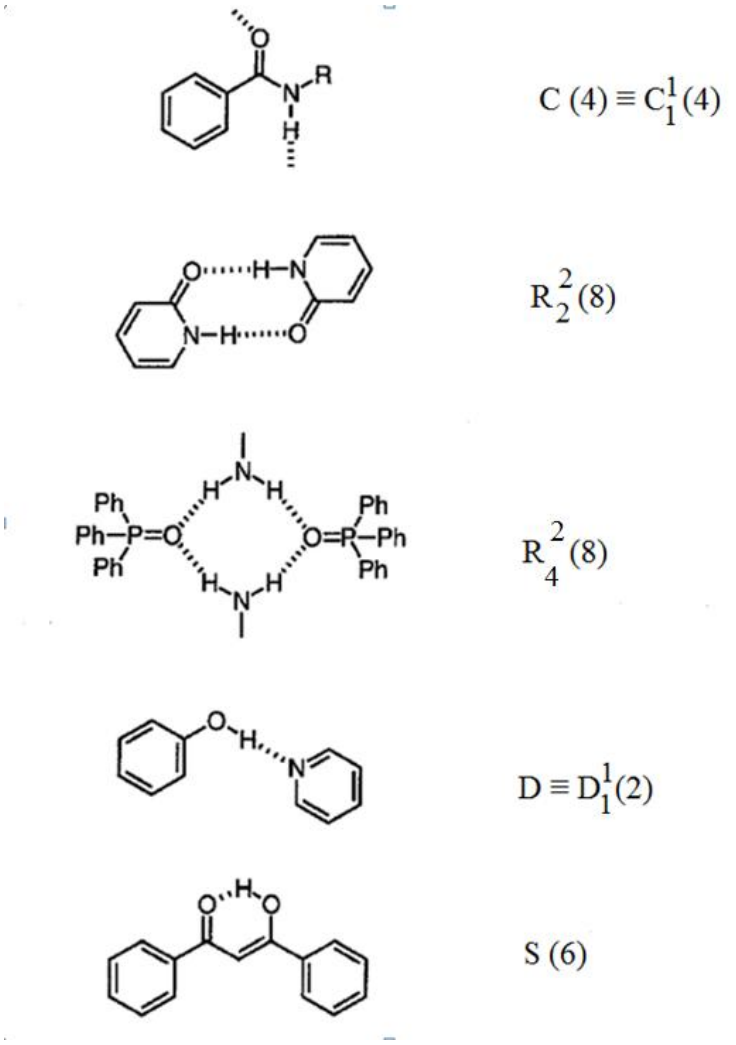

Figure 1.5 Different types of motif and their graph sets (Whitesell, 1999)

1.3 Crystal Growth

There are many types of methods for crystallization such as slow evaporation, slow cooling, solvent diffusion, vapor diffusion and reactant diffusion. All the samples in this research were grown by slow evaporation method.

1.3.1 Slow Evaporation

Evaporation is certainly one of the simplest techniques for crystallizing organic small molecule compounds. Choice of suitable solvent is important since it greatly affect the mechanism of crystal growth, because the solvent may be included into the crystal lattice while the crystal starts to form. The rate of crystal growth decreases by reducing the rate of solvent evaporation and cooling the solution. The solution should be kept by covering it. Purification of materials are necessary precondition for crystal growth, if there are impurities in the compound an oil is created in the bottom of the container (Holden and Morrison, 1982).

1.4 Problem Statement

Since the early twentieth century, pyridine derivatives have been commercially important. Pyridine derivatives have long been used in applications for medical drugs. In addition to bioactive ingredients, pyridines also have applications in polymers and dyes. In view of its medicinal importance, new compounds are needed to find more efficient source of medical drugs. In this thesis, twenty novel compounds were characterized by IR and NMR spectroscopy methods and the crystal structures were analyzed by single crystal X-ray crystallography.

Since many pharmaceuticals have carboxylic acid or pyridine functionalities, the proton transfer along hydrogen bonds between a carboxylic oxygen and a pyridine nitrogen atom has drawn considerable attention. Deprotonation of carboxylic acid renders it a better hydrogen bond acceptor, which in turn affects the molecular aggregation in crystals of salt.

1.5 Research Objectives

The objectives of this study are:

1. To synthesize new organic salts of 2-amino-5-methylpyridine and 2-amino-4-methylpyrimidine with carboxylic acid derivatives.
2. To characterize the organic salts by spectroscopy methods.
3. To analyze the molecular and crystal structure of 2-amino-5-methylpyridine and 2-amino-4-methylpyrimidine with carboxylic acid derivatives.
4. To analyze the intermolecular and intramolecular interactions formed in the crystal structure of the organic salts.

CHAPTER 2

LITERATURE REVIEW

2.1 Hydrogen Bonding Interactions and Supramolecular Chemistry

The interactions of hydrogen bond are the strongest of the non-covalent bond interactions and are directional. The study of bonds between ions and molecules is one of the topics at the present time (Braga and Grepioni, 1999). Investigations of intermolecular and inter-ionic bonds have great relation for the basic sciences, but are also helpful in connection with practical applications. It is clear that the recognition and assembly processes lead to the superstructure from components through intermolecular interactions. Therefore, the desired comprehensive physical and chemical properties are resulted *via* a reasonable control of these processes (Kepert and Rosseinsky, 1999).

Hydrogen bonding plays a fundamental role in biochemical process, catalytic, chemical, crystal engineering and supramolecular chemistry (Epstein and Shubina, 2002). In recent years, different kinds of hydrogen bonds have been recognized, and all types of them have been widely investigated carefully to their structural (Suresh, 2007) and spectral (Kruszynski, 2008) features.

In crystal engineering, carboxylic acids demonstrate most common functional groups since they have an H-bond donor and acceptor with a structure that leads to self-association *via* homosynthon motifs. In fact, self-association of carboxylic acids through centrosymmetric dimer or catemer motifs are well-known (Aitipamula and Nangia, 2005; Arora and Pedireddi, 2003). Furthermore, carboxylic acids are appropriate choices for multicomponent crystals because they produce stable

supramolecular heterosynthons with some different types of nitrogen-containing compounds.

The crystal structure of 2-aminopyridine nicotinic acetic reported by Jebas *et al.* (2006) consists of one protonated 2-aminopyridinium cation and one nicotinic acetate anion in asymmetric unit (Figure 2.1).

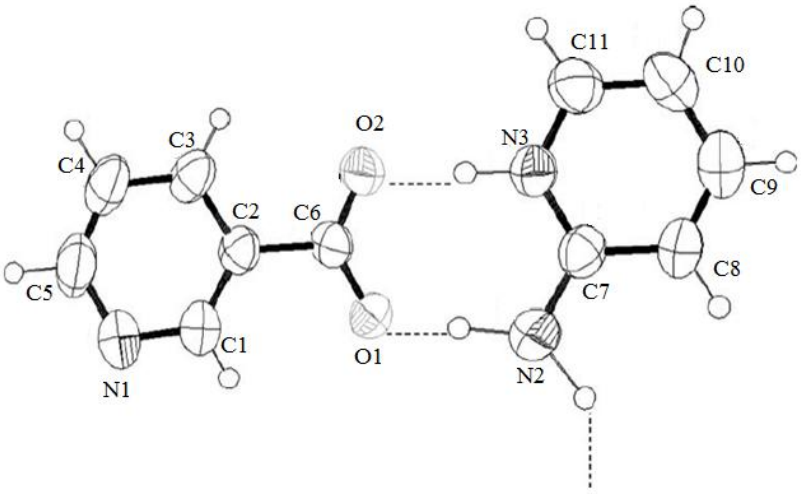

Figure 2.1 An ORTEP diagram with the atom labeling scheme. Thermal ellipsoids shown at fifty percent probability. Dashed lines represent hydrogen bonds (Jebas *et al*., 2006).

In the crystal packing (Figure 2.1), the protonated N3 atom and the 2-amino group (N2) are hydrogen-bonded to the carboxylate oxygen atoms (O1 and O2) *via* a pair of intermolecular N—H···O hydrogen bonds, creating an $R_2^2(8)$ ring motif (Bernstein *et al*., 1995).

In protonation process from carboxyl group to the 2-aminopyridine molecule, the internal angle [C11—N3—C7] was widened compared to the corresponding angle in

non-protonated 2-aminopyridine. A considerable increase in the bond length of C11—N3 and decrease in the bond lengths of N2—C7 and N3—C7 in the protonated 2-aminopyridine are observed compared to the non-protonated 2-aminopyridine, thus confirming the protonation of 2-aminopyridine at atom N3. The cation generates a pattern of fork-like hydrogen bonding with anions as depicted in Figure 2.2.

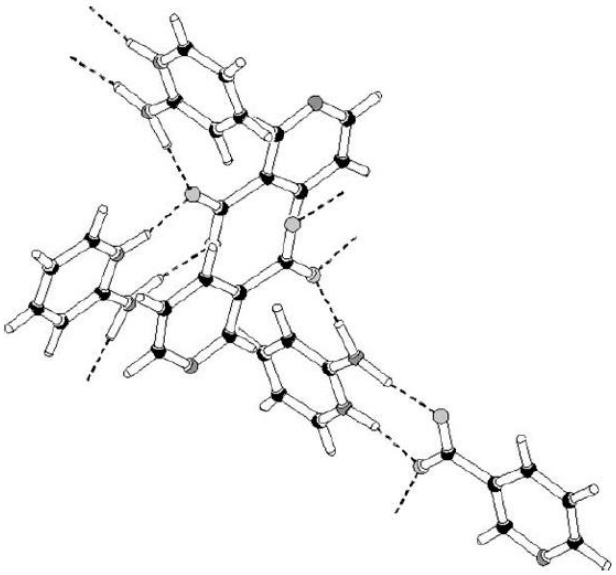

Figure 2.2 Hydrogen bonding pattern, illustrating the fork-like pattern of 2-aminopyridine nicotinic acetate (Jebas *et al*., 2006).

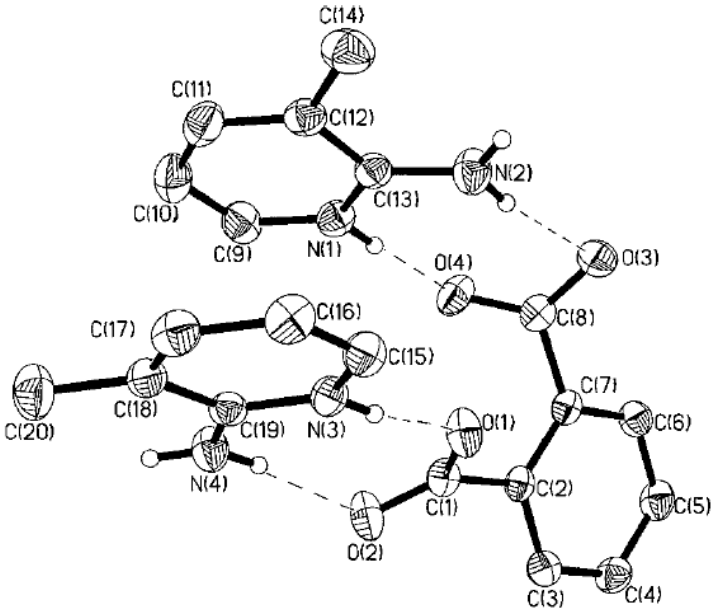

Figure 2.3 The 2-amino-3-methylpyridinium and the ortho-phthalate with atom labels, displaying fifty percent probability ellipsoids level. Dashed lines display hydrogen bonds (Jin *et al*., 2001)**.**

In the asymmetric unit of 2-amino-3-methylpyridinium ortho-phthalate (Jin *et al*., 2001; Figure 2.3), atoms N1, N3 and 2-amino groups (NH_2) act as hydrogen bond donors to atoms O3, O4, O1 and O2. The orhto-phthalic molecule is linked to a pair of 2-amino-3-methylpyridine molecules by N—H···O intermolecular hydrogen bonds to produce two eight-membered rings, each of which has the graph-set motif of $R_2^2(8)$.

The angles of C—N—C in pyridine rings are really sensitive to protonation (Boenigk, 1988; Jin, 2000) and this angle in pyridinium cation is always expanded compared to the non-protonated pyridine ring. The expansion of (C19—N3—C15) and (C13—N1—C9) indicates the type of protonated pyridine.

By studying the geometry of carboxylic group, the features of complex can be found. The average bond lengths of C–O in carboxylic group which construct hydrogen

bonds are 1.32 Å for hydroxyl (C–OH), and 1.21 (3) Å for the carbonyl bond. The average C–O bond length in the anion of carboxylate is related as 1.25 Å. The bond lengths of [C1–O1 = 1.266 Å], [C1–O2 = 1.243 Å], [C8–O3 = 1.243 Å] and [C8–O4 = 1.264 Å] confirm that proton transfer occurred from carboxylic groups to 2-amino-3-methylpyridine.

The two 2-amino-3-methylpyridinium reported by Jin *et al*. (2001) cations arranged in such way feature the existence of π–stacking interaction. It appears that the two ions with positive charge repulse each other due to electrostatic force. But, it has been proven that the atom of C (5) in 2-aminopyridine acts as an electron donator from different derivatives such as amino, imino, monocation and dication. In current structure, the atoms [N (3), N (4)] and [C (9), C (15)] are electron receiving centers and electron donating centers, respectively. The two 2-amino-3-methylpyridinium entities aligned with each other in a manner of electron receiving to donating center. This explanation is the definition of π–π interaction (Muehldorf *et al*., 1988).

He *et al.* (2010) reported that for 2-aminopyridinium and 1-phenylcyclopropane-1-carboxylate (Figure 2.4), the synthon formed is one of the four types of different synthons (Figure 2.5) between 2-aminopyridine and carboxylic acid when they form molecular complexes proposed by Bis and Zaworotko, (2005).

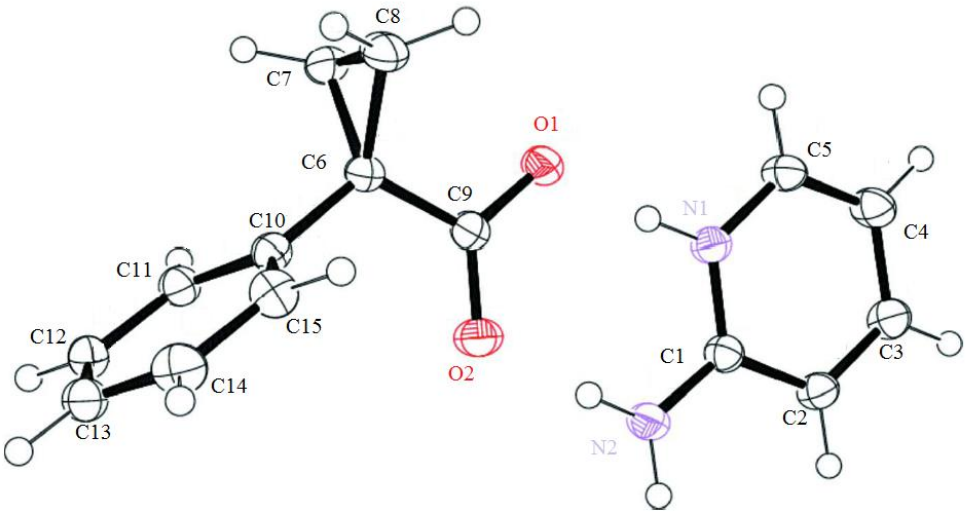

Figure 2.4 The asymmetric unit of 2-aminopyridinium and 1-phenylcyclopropane-1-carboxylate, with fifty percent probability ellipsoids level and atoms label for non-hydrogen atoms (He *et al*., 2010).

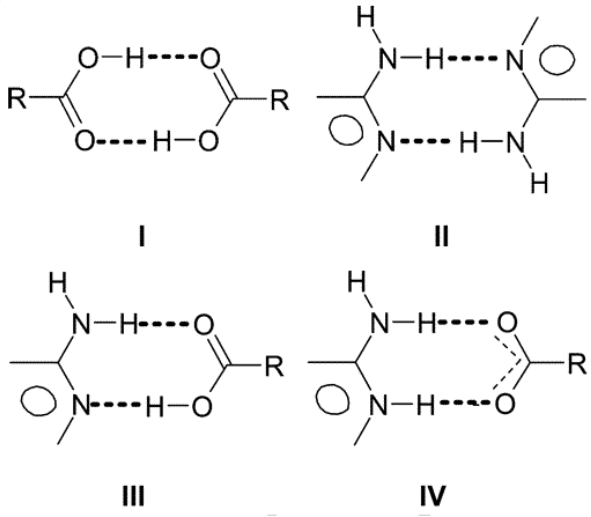

Figure 2.5 Examples of supramolecular homo and hetero synthons: A carboxylic acid homosynthon I, a 2-aminopyridine homosynthon II, 2-aminopyridine-carboxylic acid supramolecular heterosynthon III, and 2-aminopyridinium-carboxylate supramolecular heterosynthon IV (Bis and Zaworotko, 2005).

The 2-aminopyridinium cation and 1-phenylcyclopropane-1-carboxylate anion are linked through two N—H···O hydrogen bonds, forming type IV heterosynthon. These synthons are centrosymmetrically connected to generate a four-component

supramolecular *via* N—H···O hydrogen bond (Figure 2.6). The array unit is further sustained through C2—H2···π interaction [C2···Cg1 = 3.5465 (15) Å], where Cg1 is the centroid of 1-phenylcyclopropane-1-carboxylate anion (C10—C15) ring (Figure 2.6). The crystal structure is also stabilized by C11—H11···O1 (–*x*+1, –*y*+1, –*z*+1) and C12—H12···O1 (*x*+1, *y*, *z*) hydrogen bonds.

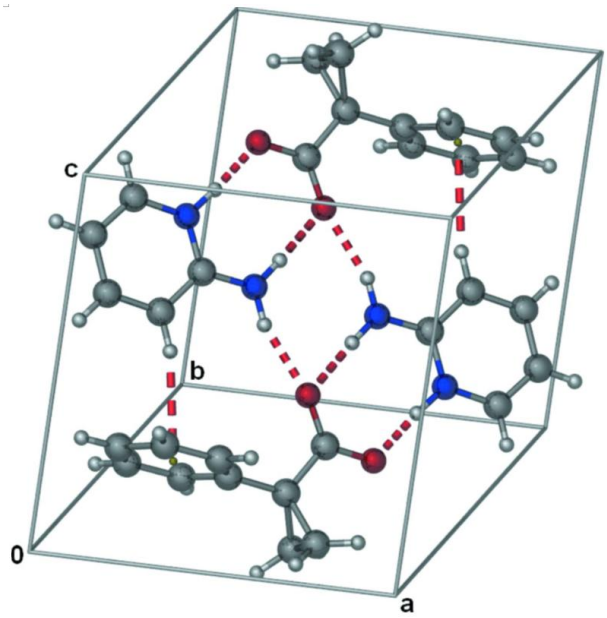

Figure 2.6 A four-component supramolecular (DDAA array) unit that illustrates of type IV heterosynthon and a C—H···π interaction in the crystal packing (He *et al.*, 2010)

2-Aminopyrimidin-1-ium trichloroacetate reported by Hu *et al.* (2002) consists of one 2-aminopyrimidinium cation and one -1-ium trichloacetate anion in asymmetric unit (Figure 2.7). In the crystal packing the protonated N atom and the amino group (NH_2) form hydrogen bonds with oxygen atoms of the carboxlate group [N^+—H···O^- and N—H···O], generating an $R_2^2(8)$ ring motif (Figure 2.7).

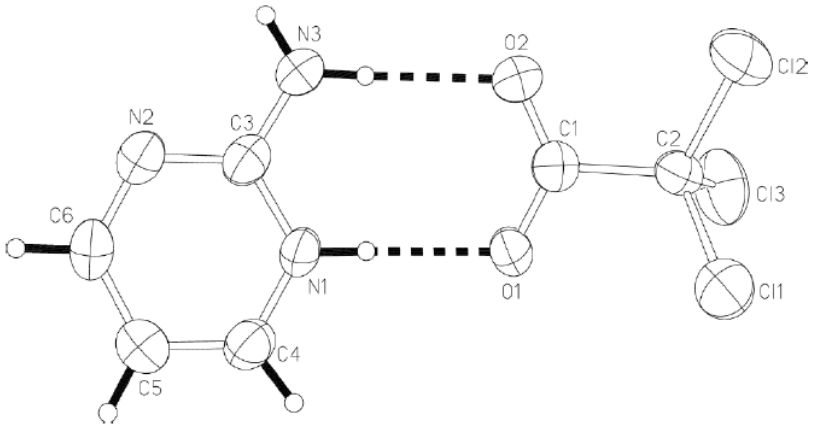

Figure 2.7 The molecular configuration and atom-numbering scheme 2-aminopyrimidin-1-ium trichloroacetate, showing fifty percent probability ellipsoids (Hu, 2002).

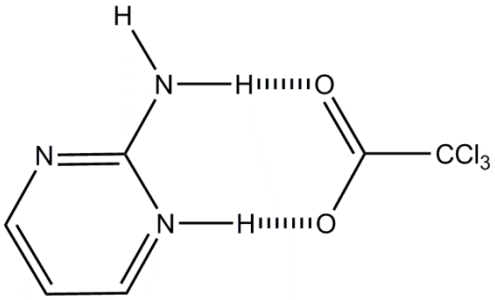

Figure 2.8 Hydrogen bonding interactions in the title salt (Hu, 2002).

Four possible motifs of 2-amino-4-methylpyrimidinium carboxylates (Figure 2.9) are reported by Aakeröy *et al*. (2003). In the crystal structure, the ion-pairs are connected by an N—H···O hydrogen bond, substantially weaker, to create an infinite helical chain along [0 1 0] direction (Figure 2.10). The crystal structure of 2-aminopyrimidinium and one -1-ium trichloacetate displays motif III.

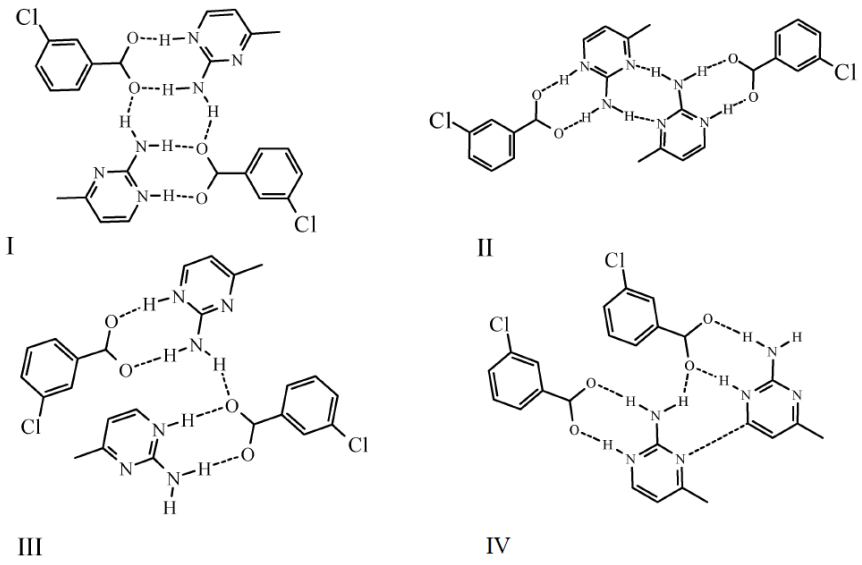

Figure 2.9 Four possible configurations for adjacent ion-pairs of 2-amino-4-methylpyrimidinium carboxylate in the crystal structures (Aakeröy *et al.*, 2003).

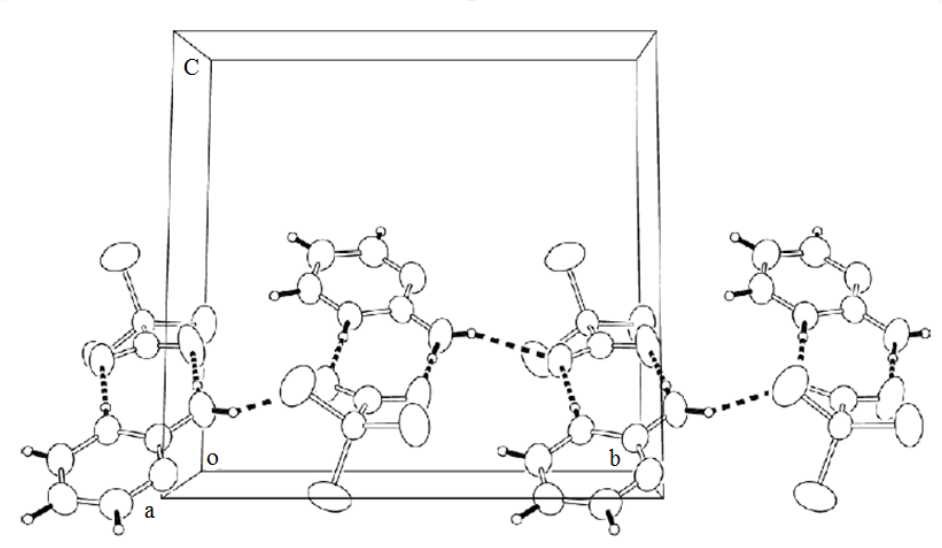

Figure 2.10 Part of the crystal structure, indicating a helical chain along the *b*-axis.

2.2 Study of Powder X-ray Diffraction (PXRD)

Adalder *et al*. (2012) reported four new co-crystals of pyrazinecarboxamide, with different types of monocarboxylic acids. The compounds are pyrazinecarboxamide - vanilic acid (PZA-VA), pyrazinecarboxamide-gallic acid (PZA-GA), pyrazinecarboxamide-1-hydroxy-2-naphthoic acid (PZA-1HNA) and pyrazinecarboxamide-indole-2-carboxylic acid (PZA-12CA). One of the characterization methods used was powder X-ray diffraction technique. Figure 2.11 illustrates that the diffractogram of product solids (bulk) and the diffractogram obtained from single crystal X–ray diffraction (SXRD) are similar to each other but are different from the diffraction pattern of the ingredient components.

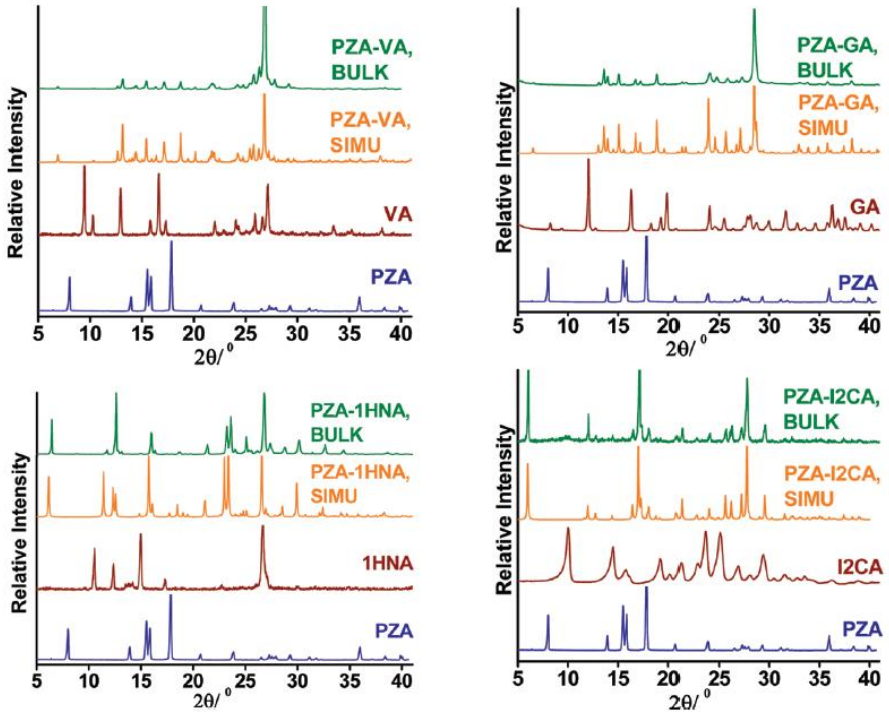

Figure 2.11 PXRD peaks of product and ingredient materials confirm a new phase (Adalder *et al*., 2012).

Four novel salts of 2-amino-4-methylpyridine, with different types of monocarboxylic acid were reported by Khalib *et al.* (2014). The reported compounds of 2-amino-4-methylpyridine 2-chlorobenzoic acid (2A4MP-2CBA), 2-amino-4-methylpyridine 2-chlorobenzoic acid (2A4MP-4CBA), 2-amino-4-methylpyridine 3-methylbenzoic acid (2A4MP-3MBA) and 2-amino-4-methylpyridine 4-methylbenzoic acid (2A4MP-4MBA) were also characterized by powder diffraction technique apart from other characterization technique. The experimental diffractogram of product solids (bulk) and the calculated diffractogram (calculated from SXRD) are similar to each other and they are different from the PXRD diffraction pattern of the starting components (Figure 2.12).

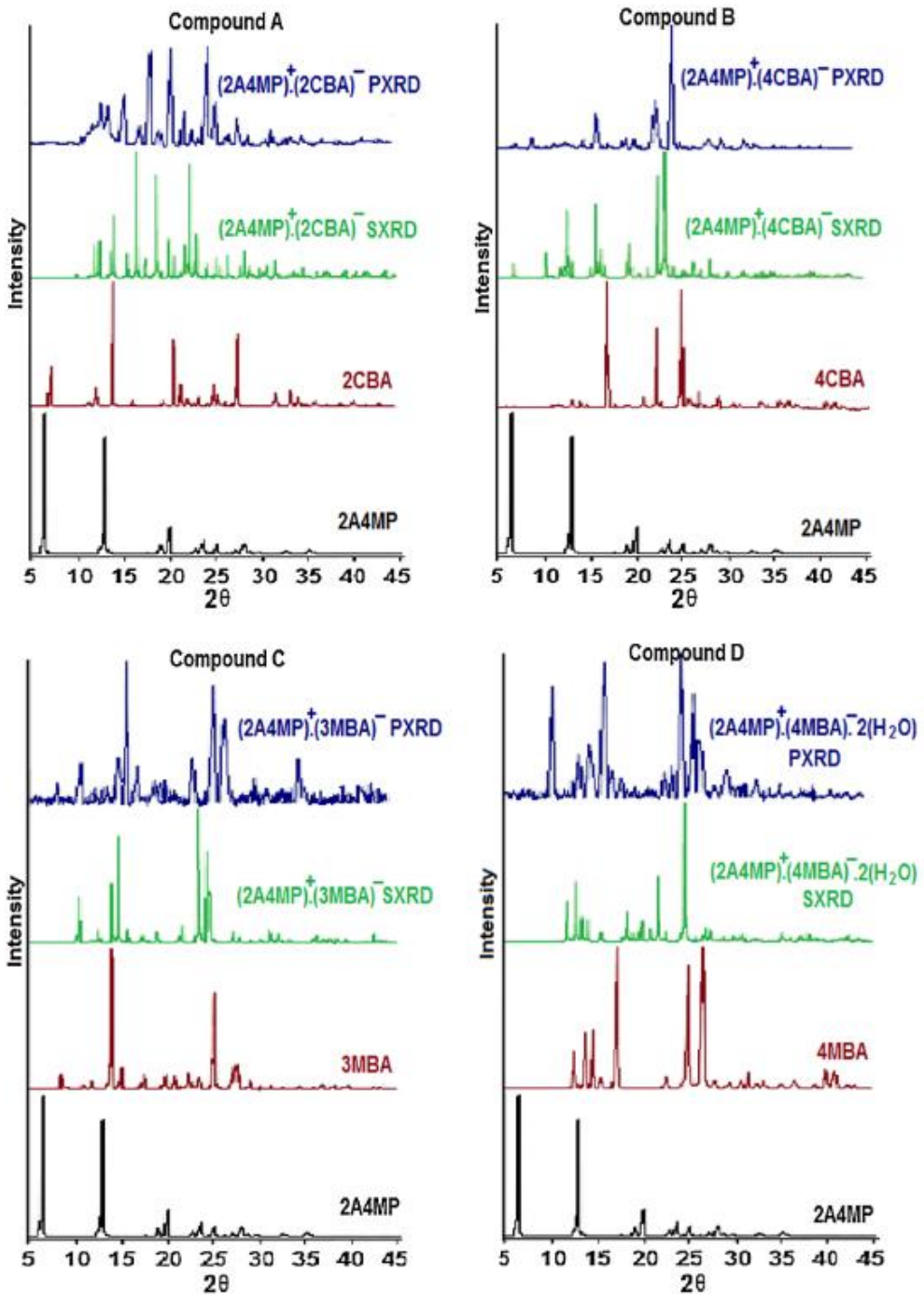

Figure 2.12 The experimental and calculated (obtained from SXRD) PXRD patterns of (2A4MP-2CBA), (2A4MP-4CBA), (2A4MP-3MBA), (2A4MP-4MBA) and their starting materials PXRD patterns (Khalib *et al.*, 2014).

2.3 Infrared Spectroscopy (IR)

Five organic salt compounds assembled from 2-aminoheterocyclic and carboxylic acid derivatives (Figure 2.13), were reported by Jin *et al*. (2011)

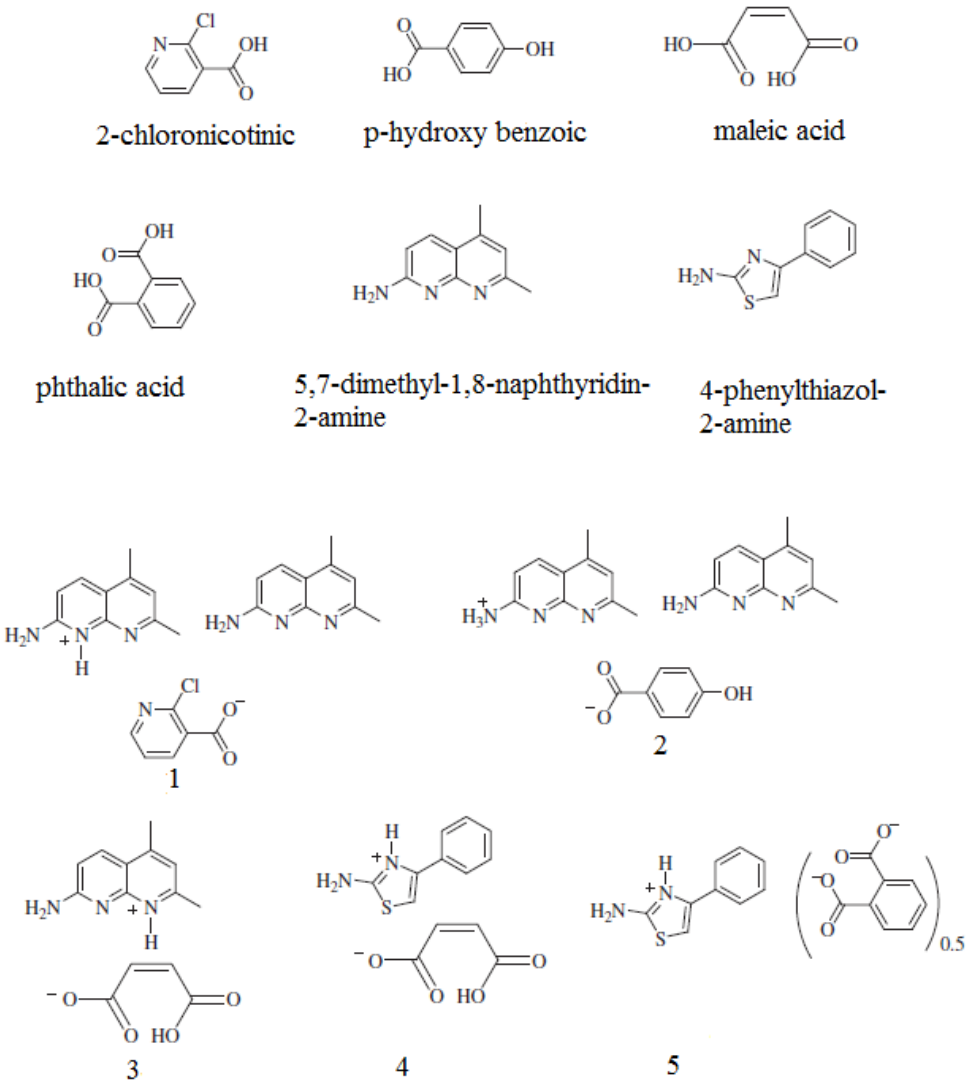

Figure 2.13 Structure of five organic salts (Jin *et al*., 2011).

Jin *et al*. (2011) reported that peaks attributed to the asymmetrical and symmetrical stretching frequencies of carboxylate ion ($–COO^-$) were found in the spectrum of the five salts. The results clearly feature that the 5, 7-dimethyl-1, 8-naphthyridine-2-amine and 4-phenylthiazol-2-amine were protonated by corresponding carboxylic acids.

Jin *et al*. (2014) have reported two organic salts assembled from banzylamine and carboxylic acid derivatives (Figure 2.14). The compounds are (benzylamine): (3,5-dinitrobenzoic acid) $[(HL^+)\cdot(dna)^-]$ (I) and $(benzylamine)_2$: $(oxalic\ acid)_2$: H_2O $[(HL^+)_2{}^{2+}\cdot(Hoxa^-)_2{}^{2-}\cdot H_2O]$ (II) (Figure 2.15).

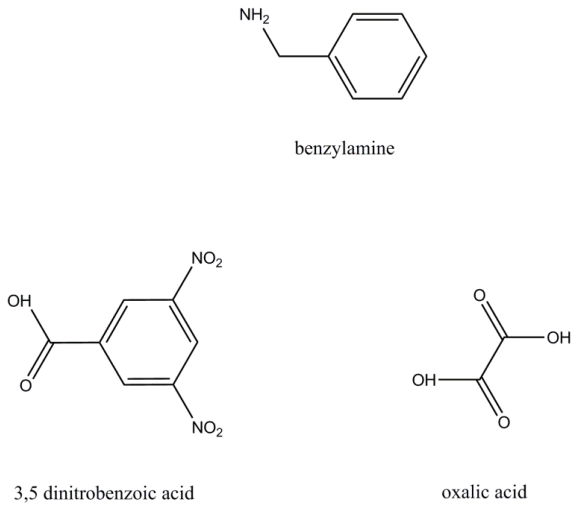

Figure 2.14 Structure of hydrogen bond synthons (Jin *et al*., 2014).

In this report by Jin *et al*. (2014), peaks attributed to the asymmetrical and symmetrical stretching frequencies of carboxylate ion ($–COO^-$) are also found in the two salts. These results also clearly show that the banzylamine was protonated by 3, 5–dinitrobenzoic and oxalic acids.